Biomarker Detection

J. K. Lee, S. R. Shin, A. Desalvo, G. Lee, J. Y. Lee, A. Polini, S. Chae, H. Jeong, J. Kim, H. Choi, H. Y. Lee*.....1700231

Nonmediated, Label-Free Based Detection of Cardiovascular Biomarker in a Biological Sample

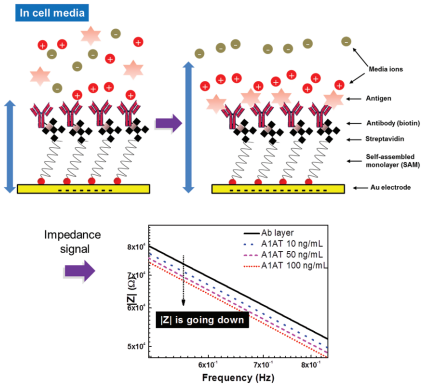

"Direct monitoring with nonmediator" is demonstrated based on impedance spectroscopy under the culture medium in order to overcome the limitation of mediator. The applicability of electrochemical monitoring is shown by detecting alpha-1-anti trypsin, which is known as biomarkers for cardiac damage and is widely chosen in organoid cardiac cell-based chip.

ADVANCED HEALTHCARE MATERIALS
www.advhealthmat.de

Nonmediated, Label-Free Based Detection of Cardiovascular Biomarker in a Biological Sample

*JuKyung Lee, SuRyon Shin, Anna Desalvo, Geonhui Lee, Jeong Yoon Lee, Alessandro Polini, Sukyoung Chae, Hobin Jeong, Jonghan Kim, Haksoo Choi, and HeaYeon Lee**

Direct electrochemical (EC) monitoring in a cell culture medium without electron transporter as called mediator is attractive topic in vitro organoid based on chip with frequently and long-time monitoring since it can avoid to its disadvantage as stability, toxicity. Here, direct monitoring with nonmediator is demonstrated based on impedance spectroscopy under the culture medium in order to overcome the limitation of mediator. The applicability of EC monitoring is shown by detecting alpha-1-anti trypsin (A1AT) which is known as biomarkers for cardiac damage and is widely chosen in organoid cardiac cell-based chip. The validity of presented EC monitoring is proved by observing signal processing and transduction in medium, mediator, medium–mediator complex. After the observation of electron behavior, A1AT as target analyte is immobilized on the electrode and detected using antibody–antigen interaction. As a result, the result indicates limit of detection is 10 ng mL^{-1} and linearity for the 10–1000 ng mL^{-1} range, with a sensitivity of 3980 nF (log [g mL])$^{-1}$ retaining specificity. This EC monitoring is based on label-free and reagentless detection, will pave the way to use for continuous and simple monitoring of in vitro organoid platform.

1. Introduction

In vitro cell studies represent a fundamental part of basic and applied research fields with large applications in healthcare, biology, and medicine.[1–10] For the last years, in vitro cell studies have been facilitated by biomarker detection which is combining with high-throughput technique as biosensor because biomarkers secreted by cells can be a sensitive indicator of pathogenic processes and pharmaceutical responses. These biomarkers are existed with small concentration within complex biological environment such as cell culture medium, biosensor should have high sensitivity and selectivity. Also continuous and long-time monitoring to evaluate the physical responses is essential point as biosensor since biomarkers are presented at minute.

In the mean time, the various analytical biosensor to assess biomarker monitoring are primarily based on immusensing by conventional enzyme-linked immunosorbent assay (ELISA) technology or mass spectroscopy.[11–14] These approaches are robust, standardized analytical tools that are difficult to integrate into cell culture systems. Moreover, these tools require time (at least few hours) to process and analyze biological samples from the cell culture systems. Recently, real-time optical methods have been developed to exploit fluorescence or surface-enhanced Raman spectroscopy and surface plasmon resonance.[14] Although the use of exogenous fluorescent compounds is required in the first case and may have potential unexpected effects on the cell culture,

Dr. J. K. Lee, Dr. H. Jeong
Department of Mechanical and Industrial Engineering
College of Engineering
Northeastern University
Boston, MA 02115, USA
Dr. J. K. Lee
National Center for Efficacy Evaluation of Respiratory Disease Product
Korea Institute of Toxicology
Jeongeup 56212, Republic of Korea
Dr. S. R. Shin, Dr. A. Desalvo, Dr. A. Polini, Dr. S. Chae
Center for Biomedical Engineering
Department of Medicine
Brigham and Women's Hospital
Harvard Medical School
Cambridge, MA 02139, USA
Dr. G. Lee
KU-KIST Graduate School of Converging Science and Technology
Korea University
Seoul 02841, Republic of Korea

DOI: 10.1002/adhm.201700231

Dr. J. Y. Lee
Department of Ophthalmology
Massachusetts Eye and Ear Infirmary
Harvard Medical School
Boston, MA 02114, USA
Prof. J. Kim, Prof. H. Y. Lee
Department of Pharmaceutical Sciences
School of Pharmacy
Bouve College of Health Science
Northeastern University
Boston, MA 02115, USA
E-mail: he.lee@neu.edu
Prof. H. Choi
Gordon Center for Medical Imaging
Department of Radiology
Massachusetts General Hospital and Harvard Medical School
Boston, MA 02114, USA
Prof. H. Y. Lee
Department of Nano-Integrated Cogno-Mechatronics Engineering
Pusan National University
Busan 46241, South Korea

Table 1. Electrochemical immunosensors reported in the literature for the determination of cardiac biomarkers (CRP, c-reactive protein; CK-MB: creatine kinase-MB, TF, transferrin; Myo, myoglobin; cTnI, cardiac troponin I; cTnT: cardiac troponin T; A1AT, alpha-1-antitrypsin; PS, polystyrene; Au, gold; MWCNTs, multiwalled carbon nanotubes; SU-8, photoresist; MB, magnetic bead; NP, nanoparticle; SPE, screen printed electrode; GNP, gold nanoparticle; ITO, indium tin oxide; EIS, electrochemical impedance spectroscopy; CV, cyclic voltammetry; DPV, differential pulse voltammetry; SWV, square wave voltammetry; PPY, polypyrrole; TMB, 3,3′,5,5′-tetramethylbenzidine; DDAB, didodecyldimethylammonium bromide; HQ, hydroquinone).

Biomarker	Electrode	Technique	*L*,*R*	LOD	Mediator	Ref.
CRP	Nanotextured PS electrode	EIS	1 pg–10 ng mL^{-1}	1 pg mL^{-1}	Electroactive polymer-PPY	[31]
CRP	Au film array electrode	Amperometry	5–48 ng mL^{-1}	1 ng mL^{-1}	TMB	[32]
CK-MB	MWCNTs embedded SU-8 hybrid nanofiber	EIS	10 ng–10 µg mL^{-1}	5 ng mL^{-1}	$K_3Fe(CN)_6$	[33]
TF	Au-MB based microfluidic sensor	Amperometry	10–4000 ng mL^{-1}	0.03 ng mL^{-1}	TMB	[34]
Myo	NP modified graphite SPE	CV, DPV, SWV	17.8–1780 ng mL^{-1}	4.4 ng mL^{-1}	Myo reduction by DDAB/Au	[35]
Myo	NP modified graphite SPE	SWV	10–400 ng mL^{-1}	5 ng mL^{-1}	Myo reduction by DDAB/Au	[36]
cTnI	GNP-ITO	Amperometry	1–100 ng mL^{-1}	1 ng mL^{-1}	HQ	[37]
cTnT	Graphite SPE	Amperometry	0.1–10 ng mL^{-1}	0.2 ng mL^{-1}	H_2O_2	[38]
A1AT	Au SPE	EIS	10–1000 ng mL^{-1}	10 ng mL^{-1}	No need mediator	This work

the latter are more focused on biomolecular interactions and suitable for a limited number of proteins.[15] Recently, electrochemical (EC) biosensors are emerged as alternative tools of conventional technology because they offer a convenient and realistic approach for the integration of analytical technology into cell culture systems.[16] This EC biosensor to detect biomarker is constituted of two major part (1) ligand layer that makes target biomarker can bind and (2) transducer, that is, converts the amount of bound biomarker into a quantitive electric signal. EC biosensor has become popular and very attractive in point-of-care devices due to their high sensitivity and ease of miniaturization.[14] They offer (i) reliability and sensitivity (e.g., 500-fold improved) far beyond conventional ELISA tests,[17] (ii) large application for the detection of biomarkers (e.g., proteins) in very small sample volumes (from 200 to 10 µL per sample in[18]), iii) multiplexing capability, and (iv) potential for integration with cell culture systems through microfluidic connections.[19–24]

Despite of considerable advantages, one of the major drawbacks of EC biosensors is the need for an EC mediator that is an electrochemical active species by redox mechanism with fast kinetics in a simple fluid (i.e., water or buffer) to perform the test to enhance the signal.[25] $K_3Fe(CN)_6$, ferrocene and methylene blue are well-known medicator in electrochemical sensor but these compounds can be cytotoxic and/or able to modify cell metabolites, leading to false results. Another problem of mediators involves real-time measurements being impossible to implement due to cells or biomolecules being unable to retain their affinity in the mediator for a long period of time. Therefore, most working biosensors separate the incubating chamber (in buffer or medium) and the measurement (in mediator) chamber.[26–30]

In this present study, the signal of the specific binding of a biomarker to the ligand layer on the electrode was measured by capacitance sensing based on electrochemical impedance spectroscopy (EIS) without an electron mediator or proton-exchange membrane. Since capacitance sensing based on the electric double layer change on the electrode by amount of adsorption of target biomarker, nor the redox reaction between electrode and biomarker, mediator's limitation can be avoid. We systematically investigated the binding of a specific biomarker to a ligand layer in cell culture medium by choosing A1AT which is known as biomarker for cardiac damage to provide an opportunity to further apply organoid cardiac cell culture system. As **Table 1** shows, most of sensor for detection of cardiac biomarker need mediator such as hydroquinone (HQ), TMB, H_2O_2.[31–38] From now, result in this manuscript is first attempt to detect cardiac marker A1AT without mediator.

Although the signal change in cell culture medium was small compared to that in a mediator, this change is sufficient for the detection of biomarkers in wider range from 10 to 10 000 ng mL^{-1}. We believed that this technique can be applied to biosensors for long-term monitoring with simplicity and high efficiency due to electron mediators not being required.

2. Results and Discussion

The SPE (screen printed electrode) consists of three electrodes (i.e., working (WE) and counter (CE) and reference (RE)). The WE and CE were deposited Au, and the RE consisted of deposited silver/silver chloride. **Figure 1** shows the impedance Bode/Nyquist plots after antibody attaching, blocking, and antigen binding in different electrolytes based on SPE. As previously mentioned, the medium contains many impurities, including bovine serum albumin. Therefore, the blocking step to prohibit nonspecific binding is performed using this medium. The Nyquist (*x*-coordinate: real component, *y*-coordinate: imaginary component) and Bode plots (*x*-coordinate: frequency, *y*-coordinate: magnitude of impedance) were expressed for sensing. The charge transfer resistance (R_{ct} expressed in Figure 1a) and magnitude (Figure 1b) below 100 Hz increased when Ag was bound to the immunolayer on the electrode. The impedance was used for observing the interfacial mechanism of the electrode. The signal in the low frequency region (<100 Hz) was dominated by the dielectric behavior of the electrode, and the resistance in solution dominated in the high frequency region.[39] Therefore, when Ag was bound to the electrode, a denser and thicker isolation layer was created, which increased the double layer resistive property.[40,41] This result is shown in

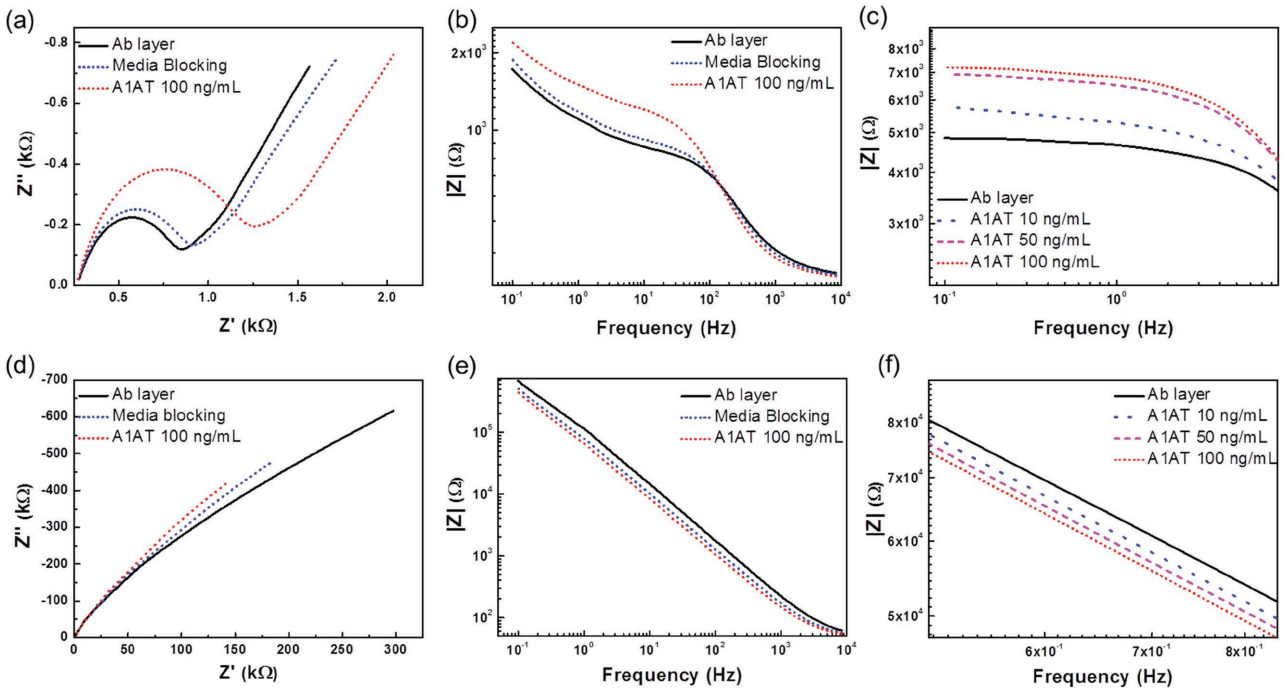

Figure 1. a,d) Impedance Nyquist and b,c,e,f) Bode plots after anti-A1AT immobilization, medium blocking, and A1AT antigen binding in 5×10^{-3} M $K_3Fe(CN)_6$ (a–c) and medium (d–f) as the electrolytes. (c) and (f) are the Bode plots after antigen immobilization with different concentrations (10, 50, and 100 ng mL^{-1}) (frequency range: (b) and (e) 0.1–1000 Hz, (c) 0.1–10 Hz, (f) 0.1–1 Hz, respectively).

Figure 1c, which shows that as the Ag concentration increases, the thickness of the isolation layer also increases. However, the opposite result was observed in the electrolyte medium. In the electrolyte medium, the mediator was not included. Therefore, no component is available to participate in the redox reaction or aid the rapid electron transfer.[42] In addition, the semisphere in the Nyquist plot was not clearly observed in medium because the charge transfer by the redox reaction is difficult compared to that in the $K_3Fe(CN)_6$ electrolyte (Figure 1d). However, some direction is shown in the Bode plot, and the magnitude of the impedance decreased when Ag is bound to the electrode below 1 kHz (Figure 1e). This result was observed when Ag was bound to the electrode at a high concentration (Figure 1f).

To fully understand the difference in the mechanism in the electrolyte medium, a set of experiments to compare the signals obtained using medium as the electrolyte solution rather than $K_3Fe(CN)_6$. The impedance Bode plot from 0.1 to 20 Hz is shown in **Figure 2**a–c. In this set of tests, different combinations were tested. First, the electrodes were tested in "pure" 5×10^{-3} M $K_3Fe(CN)_6$. Next, we characterized other sets of samples in pure medium and in mixtures of $K_3Fe(CN)_6$ and medium at various concentrations. Specific information of type of solution is explained in the Experimental Section. Interestingly, as shown in Figure 2, the trend is reversed at a higher medium concentration. For the 5×10^{-3} M $K_3Fe(CN)_6$ + 0.1× medium case, the impedance increased as the Ag concentration

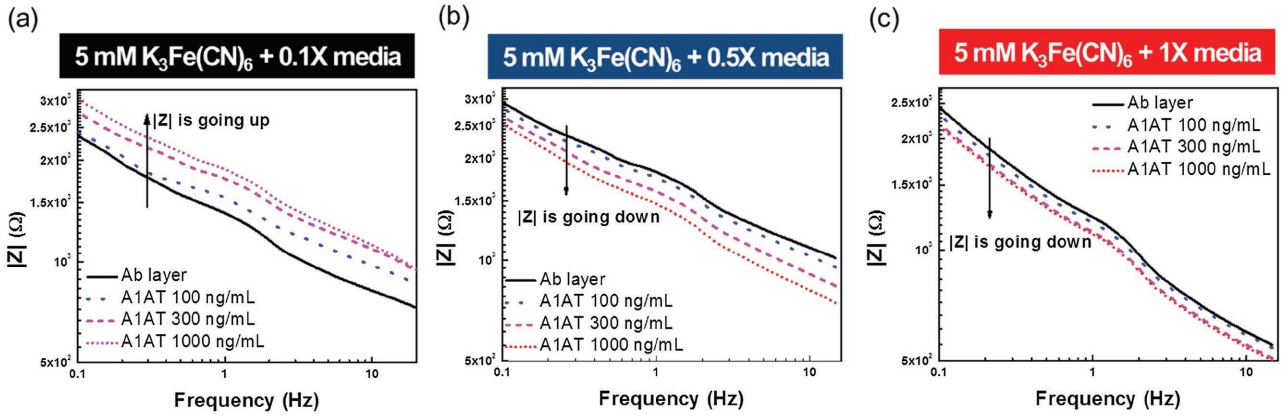

Figure 2. Bode magnitude plots after binding with A1AT (100, 300, 1000 ng mL^{-1}) in a) 5×10^{-3} M $K_3Fe(CN)_6$ + 0.1× medium, b) 5×10^{-3} M $K_3Fe(CN)_6$ + 0.5X medium, and c) 5×10^{-3} M $K_3Fe(CN)_6$ + 1× medium. The impedance was measured in a frequency range from 15 to 0.1 Hz.

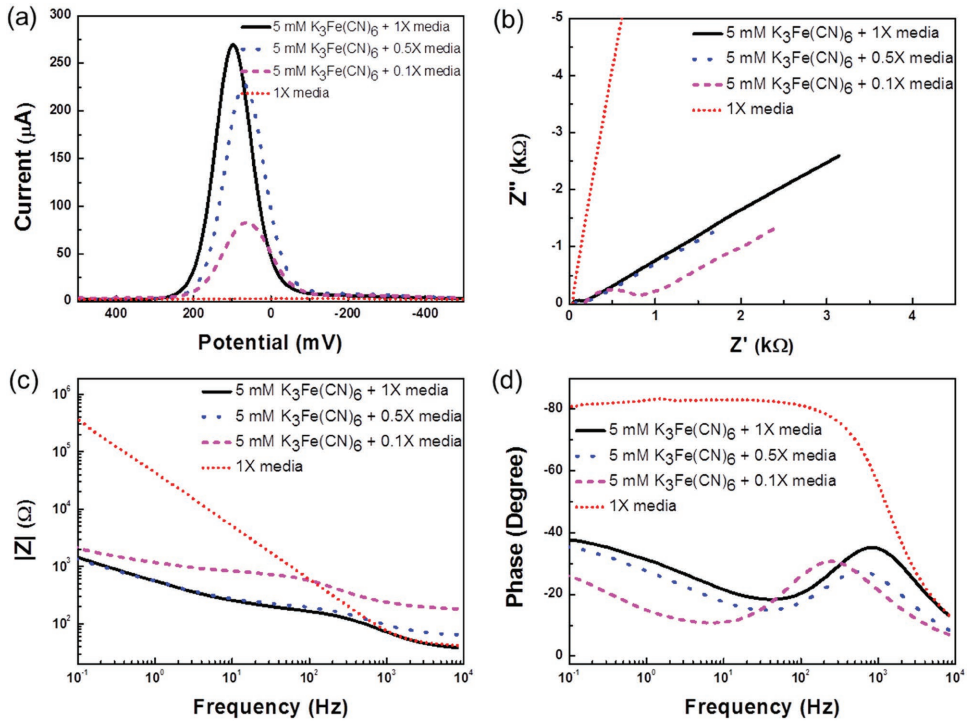

Figure 3. a) Square wave voltammetry (SWV) result. b) Impedance Nyquist plot. c) Impedance Bode plot. d) Phase diagram from the Bode plot. 5×10^{-3} M $K_3Fe(CN)_6$ + 0.1× medium, 5×10^{-3} M $K_3Fe(CN)_6$ + 0.5X medium, and 5×10^{-3} M $K_3Fe(CN)_6$ + 1× medium, 1× medium were used as the electrolytes.

increased at a specific frequency, and this trend is in agreement with the results shown in Figure 1a–c. However, the impedance started to decrease as the Ag concentration increased in the 5×10^{-3} M $K_3Fe(CN)_6$ + 0.5X medium case, and this trend was the same in 5×10^{-3} M $K_3Fe(CN)_6$ + 1× medium, although the difference was reduced. We assumed this difference was due to faradaic (redox mechanism) and non-Faradaic (charge–discharge mechanism) currents. For the sensitivity of the system, the absolute value that can be read, the higher is $K_3Fe(CN)_6$, the higher are the values due to the redox current, which enhances these results. However, if the medium concentration is increased, this redox current decreases, which facilitates the charge/discharge current. To confirm the redox current of each case, square wave voltammetry (SWV) and the entire range of the impedance graph are shown in **Figure 3**.

SWV was used to observe only the redox current that perfectly removes the charge/discharge current by a square wave potential step. The redox current was maximized in the 5×10^{-3} M $K_3Fe(CN)_6$ + 1× medium because this medium contains more cations/anions than phosphate buffered saline (PBS), which results in better facilitation of the electron movement. Therefore, the peak current gradually decreased as the concentration of the medium increased. However, no peak current was observed in pure 1× medium with no $K_3Fe(CN)_6$. This result indicates that this signal is not based on a redox reaction. Figure 3b–d shows the impedance data from 0.1 MHz to 0.1 Hz. The 1× medium result exhibits a trend/mechanism that differ from that of the other results. For the 1× medium, the magnitude of the impedance substantially increased compared to that of the other case. As shown in Figure 3d, the phase of the 1× medium was nearly –80° below 100 Hz. However, in the other graph phase, the phase is less than –40°, indicating that the impedance data in 1× medium is due to the double layer capacitance.[39,43]

Figure 4a,b is the capacitor behavior of the immunosensor in the $K_3Fe(CN)_6$ electrolyte and cell culture medium without $K_3Fe(CN)_6$. As shown in Figure 3, the oxidation and reduction is facilitated in $K_3Fe(CN)_6$, and the double layer capacitance was due to this redox reaction. In this model, $K_3Fe(CN)_6$ is used for enhancing the electron transfer because the electron transfer occurs far from the electrode surface. In addition, their rates decrease exponentially with distance.[44] If antigen was bound to the immunoaffinity layer on the electrode, their thickness (Ag–Ab complex) is changed so electron transfer of mediator is far from electrode before antigen binding. However, the capacitor behavior in cell culture medium was different compared to that with $K_3Fe(CN)_6$. We assumed that this behavior is similar to an electric double layer capacitor. In this model, the capacitance value is due to separation of charge in a Helmholtz double layer at the interface between the electrode and the electrolyte. The decrease in the capacitance can be explained by this model. The isoelectric point of anti-A1AT is 4.5–5.5, and this antibody is negatively charged in neutral medium. Therefore, the electrode surface is negatively charged, and the negatively charged medium is not attracted to the surface. If antigen bound to the immunoaffinity layer, more denser and negative charged layer is constructed, so charge distribution is more facilitated when we applied potential to the electrode. Therefore, the capacitance increased, and the impedance, which can be expressed as the barrier to pass through the electrode, decreased. To confirm this assumption, the same experiment was performed using PBS without $K_3Fe(CN)_6$. Figure 4c shows

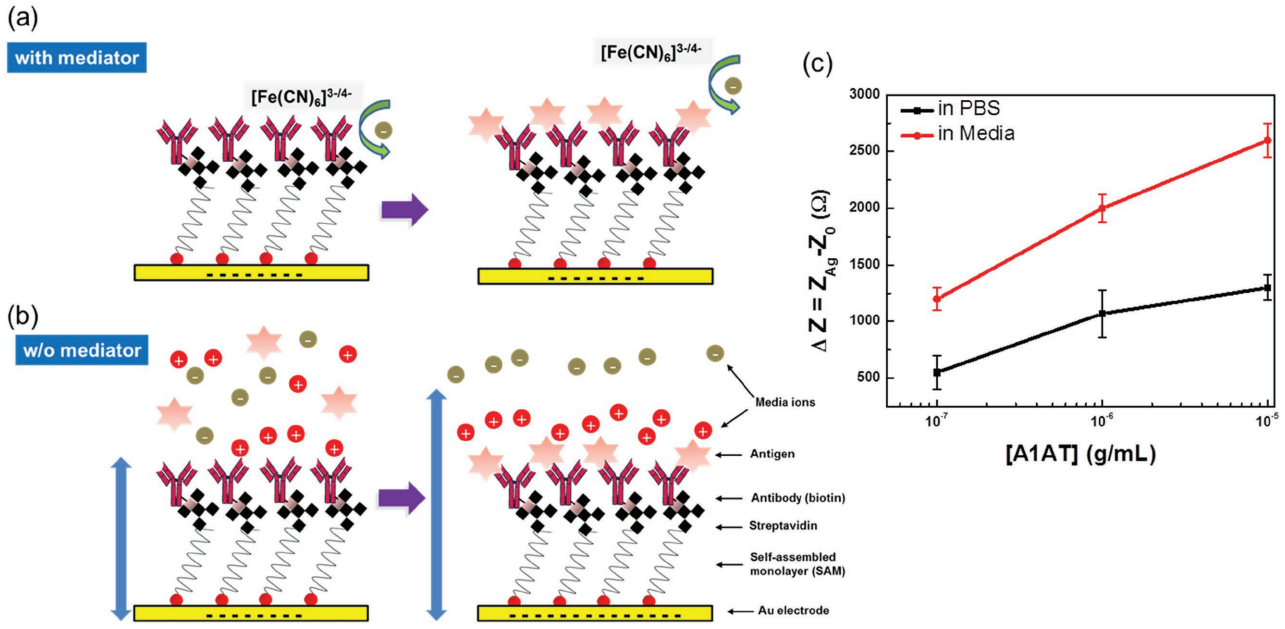

Figure 4. a) Capacitor behavior before and after attaching antigen to the immunoaffinity layer in cell culture medim + $K_3Fe(CN)_6$. b) same as (a) but capacitor behavior in cell culture medium only. c) Comparison of the relative change of the signal difference as a function of the A1AT concentration in PBS and medium as electrolyte. Both of electrolyte contain no $K_3Fe(CN)_6$. The impedance was measured at 1 Hz ($n = 5$). The self-assembled monolayer (SAM) and immunoaffinity layer act as the dielectric layer in the capacitor.

the result after immobilizing 0.1, 1, and 10 μg mL^{-1} A1AT. In this graph, the binding signal was calculated from Z_{Ag} to Z_0, where Z_{Ag} is the impedance value after specific binding of A1AT and Z_0 is the measured value prior to specific binding. Surprisingly, the impedance decreased in PBS after specific binding of A1AT. However, this difference is smaller than that in the electrolyte medium because the medium contains more cations/anions than PBS due to its higher KCl concentration (PBS: 2.7×10^{-3} M KCl, medium: 75×10^{-3} M KCl).

To demonstrate the selectivity of the measurement in cell culture medium, different concentrations of other biomarkers were added to the electrode surface to capture A1AT, which is a biomarker for cardiovascular disease. In this experiment, leptin was used as a nonspecific biomarker. In addition, we performed the EC measurement using medium because medium contains many other impurities, such as albumin, glucose, and other inorganic salts, that may interfere with obtaining an accurate binding signal for A1AT. We measured the impedance after immobilizing leptin (nonspecific) in medium (zero concentration), and the results are shown in Figure S1a,b (Supporting Information). Zero and nonspecific binding were not significantly different compared to the specific binding of A1AT. Figure S1c (Supporting Information) shows the signal change before and after immobilization of each sample (ΔZ). In this graph, the impedance signal at a frequency of 1 Hz was selected for detection, and the specific binding signal (red) was much larger than nonspecific binding (blue) and zero (black) at concentrations of 100 and 1000 ng mL^{-1}. This result indicates that our EC measurement for the immunosensor exhibits selectivity in cell culture medium without $K_3Fe(CN)_6$.

Figure 5a shows the impedance signal in cell culture medium using A1AT as specific binding for Ag. A change in the magnitude of the impedance (|Z|) was observed below 1 Hz. As shown in Figure 5a, |Z| decreased as the A1AT concentration increased. In addition, this difference is larger than the nonspecific binding signal (leptin) and zero signal, as shown in Figure S1 (Supporting Information). After the measurement, we applied the modified Randles circuit $((R_{sol})(C_{dl}[(R_{ct})(W)])(CPE))$ to the experimental data using an impedance analysis program (Z-plot), and the graph was fitted, and each value

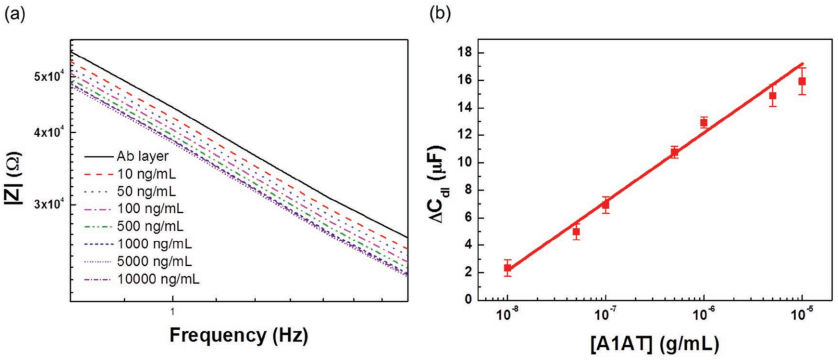

Figure 5. Bode magnitude plot after the addition of the A1AT specific antigen (from 10 to 10 000 ng mL^{-1}) to the medium. b) A1AT detection standard curve shows the relative change in capacitance as a function of the A1AT concentration. The capacitance was calculated at a frequency of 1 Hz ($n = 3$).

including the solution resistance (R_{sol}), double layer capacitance (C_{dl}), charge transfer resistance (R_{ct}), Warburg constant (W), and constant phase element (CPE) was calculated (Figure S2 and Table S1, Supporting Information).[45,46] Figure 5b shows the change in the capacitance at 1 Hz calculated from the Z-plot before and after the addition of A1AT. The equations obtained for the respective calibration graphs were as follows: ΔC_{dl} (μF) = (5.01 ± 0.32) log [A1AT] (g mL^{-1}) + (42.23 ± 2.01), (r^2 = 0.9762). In this graph, the capacitance gradually increased as the A1AT concentration increased, and a detection limit of 10 ng mL^{-1} was obtained for this nonmediator system.

Two important conclusions can be drawn from the results shown in Figure 5. As previously mentioned, the cell culture medium does not contain a mediator. Therefore, no component is present to enhance the electron transfer, and the impedance should be high at the interface between the electrode and the electrolyte.[43] In addition, in the absence of a mediator, the movement of polarized ions is dominated by the double layer capacitance rather than the electron redox reaction. This behavior was observed in the phase plot of the impedance (data not shown) because all phase degrees are nearly −90° as the A1AT concentration increased. In addition, the double layer capacitance would provide another potential avenue for detection of Ag because the Ab-Ag binding layer on the electrode will be thicker when a higher concentration of Ag is added.

3. Conclusion

A highly sensitive capacitance sensing has been developed to detect the A1AT cardiac marker. In particular, this method does not require an electron transfer mediator. Impedance spectroscopy was employed for analysis, and the double layer capacitance was calculated in this experiment. The electrical circuit model was set up in electrolyte medium, and the change in the capacitance was primarily due to charge separation in the Helmholtz layer rather than to a redox mechanism. Finally, the binding signal due to an immunological interaction with a surface-immobilized anti-A1AT antibody can be directly measured in cell medium containing various concentrations. This immune-response sensing method exhibited high sensitivity, good reproducibility, and excellent specificity. We expect that the results from this study will provide new avenues for the development of highly sensitive electrochemical sensors without redox mediators.

4. Experimental Section

Reagents and Chemicals: Potassium ferricyanide [$K_3Fe(CN)_6$] as the mediator, 11-mercaptoundecanoic acid (MUA), N-(3-dimethylaminopropyl)-*N*′-ethylcarbodimide hydrochloride (EDC), *N*-hydroxysuccinimide (NHS), and streptavidin from Streptomyces (SAv) were purchased from Sigma-Aldrich (St. Louis, USA). Dulbecco's phosphate buffered saline (DPBS) and Dulbecco's modified eagle medium (DMEM) were purchased from Life Technologies Co. (New York, USA). Active human alpha-1-antitrypsin full length protein (A1AT) as the antigen and biotinylated anti-alpha-1-antitrypsin (anti-A1AT) were provided by Abcam (Cambridge, USA).

Apparatus and Electrode: The commercial SPE (Model no: DRP-220 AT, Φ = 4 mm) were purchased from DROPSENS Co. (Kianera, Spain). It consisted of Au WE with surface area of 12.56 mm^2. This electrode includes an Au CE, and a silver pseudo-RE. All electrochemical measurements were carried out with a potentiostat/galvanostat that was obtained from CH instruments (Texas, USA, Model no: CHI 660E) at room temperature.

Preparation of the Immunoaffinity Layer: Prior to the assembly, the SPE was pretreated by placing a 50 μL drop of a 10×10^{-3} M H_2SO_4 solution, and cyclic voltammetry was performed from 0 to 1.8 V at a scan rate of 100 mV s^{-1} to remove dust. Next, SPE was washed with deionized (DI) water and dried with nitrogen. After drying in a stream of N_2, the self-assembled monolayers (SAMs) were prepared on the SPE by incubating the electrodes in 10×10^{-3} M MUA dissolved in anhydrous ethanol for 1 h at room temperature. Next, 50×10^{-3} M EDC and 50×10^{-3} M NHS in pH 5.5 sodium acetate buffer were used to activate the ester functional groups. Then, SAv (10 μg mL^{-1} in PBS) was immobilized on the SAM for 1 h at room temperature. The unreacted functional ester groups were blocked with 1 M ethanolamine for 30 min. Finally, a solution consisting of 10 μg mL^{-1} biotinylated anti-ALP was immobilized via the biotin–streptavidin affinity.

Preparation of the Electrolyte: In this study, medium and $K_3Fe(CN)_6$ were used as the electrolyte. In addition, different combinations of electrolytes were prepared to validate the capacitance calculations (i.e., (1) Pure 5×10^{-3} M $K_3Fe(CN)_6$, (2) a combination with 5×10^{-3} M $K_3Fe(CN)_6$ + 0.1× medium (40 mL of DI water, 5 mL of 50×10^{-3} M $K_3Fe(CN)_6$, and 5 mL medium), (3) 5×10^{-3} M $K_3Fe(CN)_6$ + 0.5X medium (20 mL DI water, 5 mL of 50×10^{-3} M $K_3Fe(CN)_6$, and 25 mL medium), (4) 5×10^{-3} M $K_3Fe(CN)_6$ + 1× medium (5×10^{-3} M $K_3Fe(CN)_6$ in 50 mL medium), and only (5) with 1× medium with nonmediator).

Electrochemical Impedimetric Characterization: The impedance spectra were recorded from 1 MHz to 0.1 Hz at 50 mV AC signal amplitudes. In addition, the DC potential was the same as the open circuit potential. Each decade of frequency contained 10 points. After the impedance measurement, the data were fitted for the capacitance calculation using the Z-view software from Scribner Associates Inc. (North Carolina, USA).

Supporting Information

Supporting Information is available from the Wiley Online Library or from the author.

Acknowledgements

This research was supported by the Basic Science Program of the National Research Foundation of Korea (NRF) funded by the Ministry of Education, Science and Technology (No. 2014-052607).

Conflict of Interest

The authors declare no conflict of interest.

Keywords

alpha-1-anti-trypsin (A1AT), capacitances, electrochemical impedance spectroscopy (EIS), mediator-free, screen-printed electrodes (SPE)

Received: February 20, 2017
Revised: April 17, 2017
Published online:

[1] G. Morabito, D. Trombetta, K. S. Brajendra, K. P. Ashok, S. P. Virinder, C. Naccari, F. Mancari, A. Saija, M. Cristani, O. Firuzi, L. Saso, *Biochimie* **2010**, *92*, 1101.

[2] W. Chanput, J. J. Mes, H. J. Wichers, *Int. J. Immunopharmacol.* **2014**, *23*, 37.
[3] N. Kramer, A. Walzi, C. Unger, M. Rosner, G. Krupitza, M. Hengstschläger, H. Dolznig, *Mutat. Res., Rev. Mutat. Res.* **2013**, *752*, 10.
[4] F. Nakaki, K. Hayashi, H. Ohta, K. Kurimoto, Y. Yabuta, M. Saitou, *Nature* **2013**, *501*, 222.
[5] R. Booth, H. Kim, *Lab Chip* **2012**, *12*, 1784.
[6] M. Yoon, J. L. Campbell, M. E. Andersen, H. J. Clewell, *Crit. Rev. Toxicol.* **2012**, *42*, 633.
[7] N. C. Hunt, L. M. Grover, *Biotechnol. Lett.* **2010**, *32*, 733.
[8] B. Lindroos, R. Suuronen, S. Miettinen, *Stem Cell Rev.* **2011**, *7*, 269.
[9] M. Hinchee, W. Rottmann, L. Mullinax, C. Zhang, S. Chang, *Short-Rotation Woody Crops for Bioenergy and Biofuels Applications: Biofuels*, Springer, NY, USA **2011**.
[10] A. V. Lygin, J. Upton, F. G. Dohleman, J. Juvik, O. A. Zabotina, J. M. Widholm, V. V. Lozovaya, *GCB Bioenergy* **2011**, *3*, 333.
[11] M. Stoeckli, P. Chaurand, D. E. Hallahan, R. M. Caprioli, *Nat. Med.* **2011**, *7*, 493.
[12] B. Domon, R. Aebersold, *Science* **2006**, *312*, 212.
[13] R. Aebersold, M. Mann, *Nature* **2003**, *422*, 198.
[14] C. A. Baker, C. T. Duong, A. Grimley, M. G. Roper, *Bioanalysis* **2009**, *1*, 967.
[15] K. N. Han, C. A. Li, G. H. Seong, *Annu. Rev. Anal. Chem.* **2013**, *6*, 119.
[16] A. Hasan, M. Nurunnabi, M. Morshed, A. Paul, A. Polini, T. Kulia, M. A. Hariri, Y. K. Lee, A. A. Jaffa, *Biomed. Res. Int.* **2014**, *2014*, 18.
[17] L. Wang, W. Chen, D. Xu, B. S. Shim, Y. Zhu, F. Sun, L. Liu, C. Peng, Z. Jin, C. Xu, N. A. Kotov, *Nano Lett.* **2009**, *9*, 4147.
[18] J. W. Choi, K. W. Oh, J. H. Thomas, W. R. Heineman, H. B. Halsall, J. H. Nevin, A. J. Helmicki, H. T. Henderson, C. H. Ahn, *Lab Chip* **2002**, *2*, 27.
[19] M. Pumera, S. Sanchez, I. Ichinose, J. Tang, *Sens. Actuators, B* **2007**, *123*, 1195.
[20] C. A. Holland, F. L. Kiechle, *Curr. Opin. Microbiol.* **2005**, *8*, 504.
[21] A. Weltin, K. Slotwinski, J. Kieninger, I. Moser, G. Jobst, M. Wego, R. Ehfet, G. A. Urban, *Lab Chip* **2014**, *14*, 138.
[22] S. C. Shih, I. Barbulovic-Nad, X. Yang, R. Fobel, A. R. Wheeler, *Biosens. Bioelectron.* **2013**, *42*, 314.
[23] K. F. Lei, M. H. Wu, C. W. Hsu, Y. D. Chen, *Biosens. Bioelectron.* **2014**, *51*, 16.
[24] T. A. Nguyen, T. I. Yin, D. Reyes, G. A. Urban, *Anal. Chem.* **2013**, *85*, 11068.
[25] S. Choi, M. Goryll, L. Y. M. Sin, P. K. Wong, J. Chae, *Microfluid. Nanofluid.* **2011**, *10*, 231.
[26] K. Blagovic, L. Y. Kim, J. Voldman, *PLoS One* **2011**, *6*, e22892.
[27] R. H. Liu, M. J. Lodes, T. Nguyenm, T. Siuda, M. Slota, H. S. Fuji, A. McShea, *Anal. Chem.* **2006**, *78*, 4184.
[28] P. Bombelli, T. Müller, T. W. Herling, C. J. Howe, T. P. Knowles, *Adv. Eng. Mater.* **2015**, *5*, 1.
[29] S. Srivastava, M. A. Ali, P. R. Solanki, P. M. Chavhan, M. K. Pandey, A. Mulchandani, A. Srivastava, B. D. Malhotra, *RSC Adv.* **2013**, *3*, 228.
[30] P. Truman, P. Uhlmann, M. Stamm, *Lab Chip* **2006**, *6*, 1220.
[31] V. Kunduru, M. Bothar, J. Grosch, S. Sengupta, P. K. Patra, S. Prasad, *Nanomedicine* **2010**, *6*, 642.
[32] J. K. Lee, G. Yoo, M. Park, J. Jose, M. J. Kang, J. C. Pyun, *Sens. Actuators, B* **2012**, *175*, 46.
[33] M. D. Prakash, S. G. Singh, C. S. Sharma, V. S. R. Krishna, *Electroanalysis* **2016**, *28*, 1.
[34] R. Riahi, S. A. M. Shaegh, M. Ghaderi, Y. S. Zhang, S. R. Shin, J. Aleman, S. Massa, D. Kim, M. R. Dokmeci, A. Khademhosseini, *Sci. Rep.* **2016**, *6*, 24598.
[35] V. V. Shumyantseva1, T. V. Bulko, M. Yu. Vagin, E. V. Suprun, A. I. Archakov, *Biochemistry (Moscow) Suppl. Ser. B: Biomed. Chem.* **2010**, *4*, 237.
[36] E. V. Suprun, A. L. Shilovskaya, A. V. Lisitsa, T. V. Bulko, V. V. Shumyantseva, A. I. Archakov, *Electroanalysis* **2011**, *23*, 1051.
[37] A. J. S. Ahammad, Y. H. Choi, K. Koh, J. H. Kim, J. J. Lee, M. Lee, *Int. J. Electrochem. Sci.* **2011**, *6*, 1906.
[38] B. V. M. Silva, I. T. Cavalcanti, A. B. Mattos, P. Moura, M. D. P. T. Sotomayor, R. F. Dutra, *Biosens. Bioelectron.* **2010**, *26*, 1062.
[39] L. Yang, Y. Li, C. L. Griffis, M. G. Johnson, *Biosens. Bioelectron.* **2004**, *19*, 1139.
[40] J. K. Lee, G. H. Noh, J. C. Pyun, *Biochip J.* **2009**, *3*, 287.
[41] J. Lee, S. Cho, J. Lee, H. Ryu, J. Park, S. Lim, B. Oh, C. Lee, W. Huang, A. Busnaina, H. Lee, *J. Biotechnol.* **2013**, *168*, 584.
[42] M. B. Achari, V. Elumalai, N. Vlachopoulos, M. Safdari, J. Gao, J. M. Gardner, L. Kloo, *Phys. Chem. Chem. Phys.* **2013**, *15*, 17419.
[43] G. Y. Lee, Y. H. Choi, H. W. Chung, H. Ko, S. Cho, J. C. Pyun, *Biosens. Bioelectron.* **2013**, *40*, 227.
[44] F. A. Armstrong, G. S. Wilson, *Electrochim. Acta* **2000**, *45*, 2623.
[45] S. Cho, H. Thielecke, *Biosens. Bioelectron.* **2007**, *22*, 1764.
[46] S. Carrara, L. Benini, V. Bhalla, C. Stagni, A. Ferretti, A. Cacallini, B. Ricco, B. Samorì, *Biosens. Bioelectron.* **2009**, *24*, 3425.

